Available online at www.sciencedirect.com
SCIENCE DIRECT®
Optics Communications 255 (2005) 319–330
OPTICS COMMUNICATIONS
www.elsevier.com/locate/optcom

Performance simulation for ferroelectric thin-film based waveguide electro-optic modulators

De-Gui Sun [a,b], Zhifu Liu [a,*], Yingyan Huang [a], Seng-Tiong Ho [a], David J. Towner [c], Bruce W. Wessels [c]

[a] *Department of Electrical and Computer Engineering, Northwestern University, 2145 Sheridan Road, Evanston, IL 60208, USA*
[b] *State Key Laboratory of Applied Optics, Changchun Institute of Optics, Fine Mechanics and Physics, Chinese Academy of Sciences, Changchun 130031, China*
[c] *Department of Materials Science and Engineering and Materials Research Center, Northwestern University, Evanston, IL 60208, USA*

Received 9 August 2004; received in revised form 14 March 2005; accepted 13 June 2005

Abstract

We simulate thin-film based electro-optic modulator structures to target low drive voltage, high-speed modulation, and small device size by using $BaTiO_3$ ferroelectric film as an exemplary device material with optimizing film thickness. The calculations are performed for both the case of an experimental film having $r_{eff} = 35$ pm/V and the case of an ideal thin-film having $r_{51} = 730$ pm/V. For the case of $r_{51} = 730$ pm/V, a new relation between the drive voltage and the interaction length is derived with respect to the special configuration of $BaTiO_3$ thin-films. For the optimal case of the film thickness and the waveguide design, the frequency–voltage-size performances that can be achieved include: >2.5 GHz with 0.75 V V_π and 31.1 mm length, 10 GHz with 1.5 V V_π and 7.8 mm length, > 40 GHz with 3.0 V V_π and 1.9 mm length, and > 100 GHz with 4.8 V V_π and 0.8 mm length. Various physical factors unique to the frequency–voltage-size performance trade-off of the thin-film EO modulator structures are discussed.

Keywords: Electro-optic modulator; Quadratic EO relation; Optical waveguide; $BaTiO_3$ thin-film; Frequency response; Characteristic impedance; Microwave propagation loss

1. Introduction

High-speed optical intensity modulators based on ferroelectric crystals are important in optical communication networks because of their linear response and low frequency chirping. In particular, waveguide electro-optic (EO) modulators based on $LiNbO_3$ have been the most widely used in the industry. Current interests in ferroelectric modulator device technologies include the realization of higher speed (~40 GHz), lower driving

* Corresponding author. Tel./fax: +1 847 467 2169.
E-mail address: z-liu3@northwestern.edu (Z. Liu).

0030-4018/$ - see front matter © 2005 Elsevier B.V. All rights reserved.
doi:10.1016/j.optcom.2005.06.028

voltage (~1 V), and smaller device size [1]. High speed requires the EO modulator to have a large 3 dB frequency response. A lower switching voltage can be achieved by using a non-linear material with a larger EO coefficient. For high-speed operation, various design factors have to be considered. First is the velocity matching between the optical signal and the traveling RF signal, the second is the interaction length between the RF and optical signals, and the third is the characteristic impedance matching between the driving microwave electrode and the external electronic signal generator. Ferroelectric materials with high EO coefficients typically have high dielectric constants as well, resulting in a large phase velocity mismatch and low modulation frequency in spite of their shorter device length.

Electro-optic modulator technologies based on $LiNbO_3$ waveguides have been pushed close to their performance limits using special techniques including ridge structures, buffer layers, and the shielding plane to achieve better velocity matching and other requirements for high-speed operations [2–4]. EO modulators having modulation bandwidths of higher than 40 GHz are receiving extensive research interest. The intrinsic EO coefficient of $LiNbO_3$ ($r_{33} = 31$ pm/V) and its microwave attenuation due to both conductor and dielectric propagation losses are the main factors limiting the 3 dB frequency response of $LiNbO_3$ modulators to 40 GHz modulation frequency at about 5 V switching voltage with device lengths of 2–4 cm [1–4]. In this paper, we show that with use of a thin-film structure it is possible to lower the effective dielectric constant of the RF wave and increase the operational bandwidth. We explore the case of a ferroelectric material possessing a much larger EO coefficient than $LiNbO_3$, and achieve lower effective dielectric constant of the RF wave, lower switching voltages, and relatively high modulation frequencies and short device lengths. As a specific numerical example, we take the case of barium titanate ($BaTiO_3$) as the high EO coefficient material [5,6]. In terms of increasing modulation bandwidth and shortening device size (or lowering modulating voltage), thin-film ferroelectric materials have additional degrees of freedom to achieve performance optimization over their bulk forms. Recently, EO modulators based on $BaTiO_3$ thin-films have been demonstrated with straight waveguide phase modulation structures [7,8], and Mach-Zehnder interferometer (MZI) type intensity modulation structures [9,10]. While the initial demonstration has not quite achieved the material parameters of an ideal $BaTiO_3$ thin-film, it showed the feasibility of such a modulator structure. It is thus of interest to explore how the variation of the thin-film EO modulator structure would affect the modulation voltage and bandwidth, thereby leading to certain optimal design depending on application requirements.

2. Optimization for low drive voltage and short interaction length

2.1. General discussion

The challenge for the next generation of EO modulators is to simultaneously achieve low modulation voltage (or small device size) and fast modulation speed. $BaTiO_3$ has a large EO coefficient and is capable of being grown as thin-films up to several microns in thickness on MgO substrates [7,8]. In Fig. 1, we show a schematic of a waveguide EO intensity modulator using a *c*-axis $BaTiO_3$ film grown on an MgO substrate with a coplanar RF waveguide (CPW) structure for the propagating RF signal. The middle electrode is the ground. One of the two side electrodes carries the drive voltage, and the other side electrode is used for

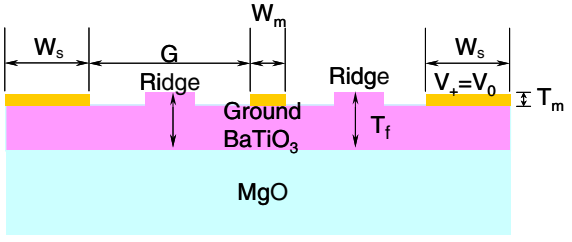

Fig. 1. Schematic of the Mach-Zehnder waveguide EO intensity modulator using a $BaTiO_3$ films on MgO substrate with CPW electrodes, W_s = side electrode width, G = gap size between electrodes, W_m = middle electrode width (at ground), T_m = electrode thickness, V_0 = modulation voltage, where the middle one is for the ground and one side electrode is for the drive signal, and the other one is used for reference.

reference purpose. In this device geometry, the electric field is applied along the x-axis and the optical beam propagates along the y-axis. $BaTiO_3$ belongs to crystal symmetry class 4 mm, and its electro-optic tensor has five non-zero components: r_{13}, r_{23}, r_{33}, r_{42}, r_{51}, with relations of $r_{13} = r_{23}$, $r_{51} = r_{42}$. In Fig. 1, the external electric field is applied along the x-axis. Therefore, only r_{51} is involved. The EO modulation of refractive index has a quadratic relation with r_{51} and external electric field E as [11]

$$\Delta n = \frac{n_o^3 r_{51}^2 E^2}{2\left(\frac{1}{n_e^2} - \frac{1}{n_o^2}\right)}, \tag{1}$$

where n_o and n_e are the optical refractive indices of ordinary and extraordinary light waves, respectively. Now we still define the drive voltage that can produce a half-wave phase change as V_π. Then, with Eq. (1), we have a relation between the half-wave drive voltage V_π and the interaction length L in the modulation case as

$$V_\pi^2 L = \frac{\lambda G^2 (n_o^2 - n_e^2)}{n_o^5 n_e^2 r_{51}^2 \Gamma^2}, \tag{2}$$

where λ is the optical wavelength, G is the electrode gap, n is the optical refractive index of the EO material, L is the interaction length between the optical and RF signals, and Γ is the overlap integral factor of the optical and the RF electric fields given by [12]

$$\Gamma = \frac{G}{V} \frac{\int\int E_e |E_o|^2 \, dx \, dz}{\int\int |E_o|^2 \, dx \, dz}, \tag{3}$$

where E_e and E_o are the amplitudes of electric field and optical field, respectively. Note from Eq. (2) that the large r_{51} of $BaTiO_3$ provides an intrinsic advantage for achieving a low $V_\pi^2 L$ value. Furthermore, a small G and a large Γ will be conducive for further minimizing $V_\pi^2 L$. Further note from Eq. (2) that the relation between wavelength λ and $V_\pi^2 L$ is still linear, but all other parameters: G, Γ, n_o and n_e are higher powered.

2.2. Optical field discussion

For practical EO modulator applications, low optical insertion loss is important. The optical absorption induced by the metal electrodes could be a dominant source of optical loss if the optical field has substantial energy at the electrodes. Thus, the electrodes shown in Fig. 1 must be placed far away from the waveguide channels to prevent the light from incurring substantial absorption due to the electrodes. This contradicts the requirement for a small gap G between two electrodes, as indicated by Eq. (2). For our purpose here, the effective size of the optical mode of interest is defined as the distance of the points where the electric field amplitude of the optical mode is at 5% of its peak value, and the optical power at this point is 0.25% of its peak value. The half-width of the effective size will be referred to as half-width at 5% and expressed as $W_{D5\%}$. Because the device length is much shorter than the counterpart of $LiNbO_3$ based devices, the optical power absorption by the metal electrodes is not so high as that of the longer $LiNbO_3$ based devices. We only require the electrodes to be located at the half-width (i.e. $W_{D5\%}$) or further away from the mode center, $G \geqslant 2W_{D5\%}$. Consequently, in order to have the EO modulator system satisfying the requirements of low optical loss and low $V_\pi^2 L$ product defined by Eq. (2), parameter $W_{D5\%}$ should be as small as possible for small mode size. As will be seen below, it turns out that while $G \geqslant 2W_{D5\%}$ is more than sufficient to reduce the electrode metal-induced optical loss to a negligible value, the lower limit of gap G is further restricted by the requirement of matching with 50 Ω transmission line impedance. This requires G to be even wider than $2W_{D5\%}$. In the regime, we are discussing here, because a CPW is employed (Fig. 1), only the horizontal component of the RF electric field (E_x) is of interest. A coordinate system and the device geometry are presented in Fig. 2. In Fig. 2, W_r is the width of the ridge waveguide and the coordinates are defined by the x-, y- and z-axes as shown.

In this study, we assume that the $BaTiO_3$ film is epitaxial on an MgO (100) substrate and that the film consists of a single ferroelectric domain with polarization normal to the film surface. The optical constants for this system are taken as the typical values for $BaTiO_3$ crystal at the

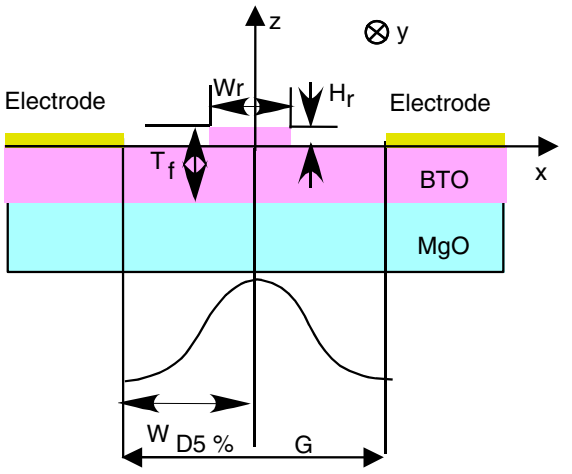

Fig. 2. Relation between the half-width at 5% maximum optical field $W_{D5\%}$ and the electrode gap G. In the figure, W_r and H_r indicate the width and the height of ridge, respectively, and T_f the film thickness. The zero point of z-axis is set at the interface between the electrode and the thin-film.

wavelength of 1.55 μm, for which the ordinary and extraordinary refractive indices are given by $n_o = 2.289$ and $n_e = 2.282$, respectively, the microwave constants are taken as $\varepsilon_x = 2200$ and $\varepsilon_z = 56$ [6], and the optical refractive index and the microwave dielectric constant of MgO material are taken as 1.7147 and 8.1, respectively [13]. We calculate the $W_{D5\%}$ for six different $BaTiO_3$ film thickness, (0.5, 1.0, 2.0, 3.0, 4.0, and 5.0 μm) to obtain the relation between the $W_{D5\%}$ and the ridge width (W_r) by selecting a fixed ratio of 0.4 between the ridge height and the film thickness ($H_r/T_f = 0.4$) and by considering the regime where the waveguide supports near single optical mode horizontally. Near single mode means up to 2 possible modes in which it is still easy to excite mainly the fundamental mode since the second mode has odd symmetry for its electric field (fundamental mode has even symmetry) and is relatively far away from the fundamental mode in terms of wave-guiding angle. These assumptions are for the purpose of exploring parameter space. Actual design will depend on applications (e.g., pure single mode may be needed for stringent applications). Multimode below will refer to waveguides that support more than two guided modes. The obtained data for the six film

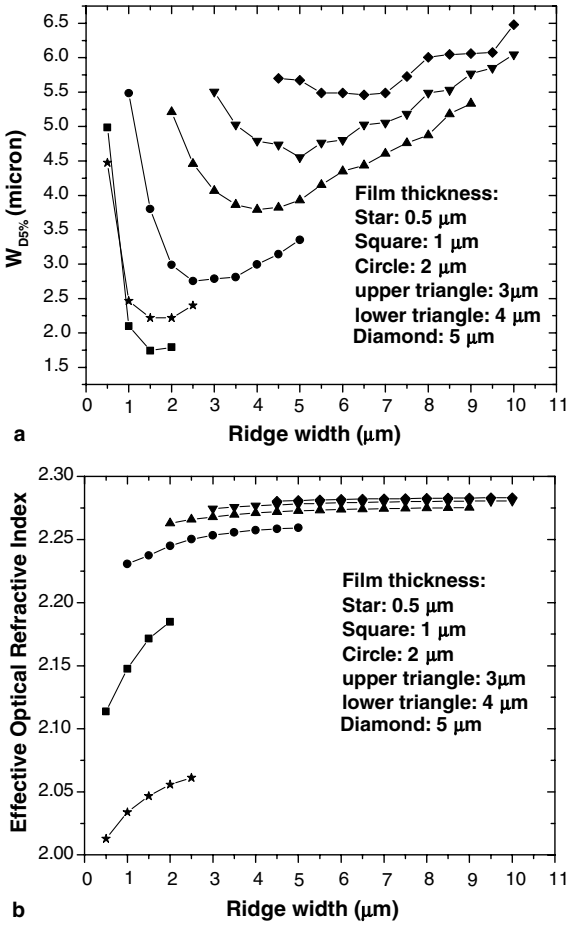

Fig. 3. (a) $W_{D5\%}$ (half-width at 5%) vs. ridge width. (b) The effective optical refractive index vs. ridge width for six different values of film thickness: 0.5, 1.0, 2.0, 3.0, 4.0, and 5.0 μm. $H_r/T_f = 0.4$ for 1.0–5.0 μm thick films; $H_r/T_f = =0.2$ for 0.5 μm thick film.

thickness values are presented graphically in Fig. 3, where Fig. 3(a) is for $W_{D5\%}$ vs. W_r and Fig. 3(b) for the optical effective refractive index of the propagating optical beam vs. W_r.

Note from Fig. 3 that there is always a smallest value of $W_{D5\%}$ for each film thickness, which is the optimal point of this regime. We will refer to these optimal points for the six film thickness values as the optimal waveguide designs below. We summarize the waveguide parameters for these optimal points in Table 1. In Table 1, parameters related to $W_{D5\%}$ are listed and include the ridge width, the optical effective refractive index, and the mode

Table 1
Optimal waveguide design parameters for the six values of $BaTiO_3$ film thickness: 0.5–5.0 μm

Items	0.5 (μm)	1.0 (μm)	2.0 (μm)	3.0 (μm)	4.0 (μm)	5.0 (μm)
Ridge width (μm)	1.5	1.5	2.5	4.0	5.0	6.5
$W_{D5\%}$ (μm)	2.219	1.743	2.754	3.794	4.552	5.461
N_{op}	2.0466	2.1714	2.2503	2.2711	2.2782	2.2821
Mode depth D_{md} (μm)	0.170	0.209	0.276	0.350	0.409	0.507

depth (D_{md}). The mode depth D_{md} is defined in Fig. 4 and is used for expressing how deep the optical mode center is from the top surface of the $BaTiO_3$ film where the electrodes are deposited. This parameter also affects the value of the overlap integral factor between the microwave electric field and the optical field. The closer to the top surface of the $BaTiO_3$ film the mode center is, the higher the overlap integral factor Γ. Further note from Table 1 that the optical effective refractive index is larger in a thicker film than in a thinner film. In practice, the vertical optical mode size shall also meet the condition that its $W_{D5\%}$ point at the surface side be away from the surface of the $BaTiO_3$ film to minimize optical loss. This consideration would be dependent on the actual quality of the film surface and ridge sidewalls. Note from Table 1 that the mode center gradually goes down with increasing thickness of the $BaTiO_3$ films.

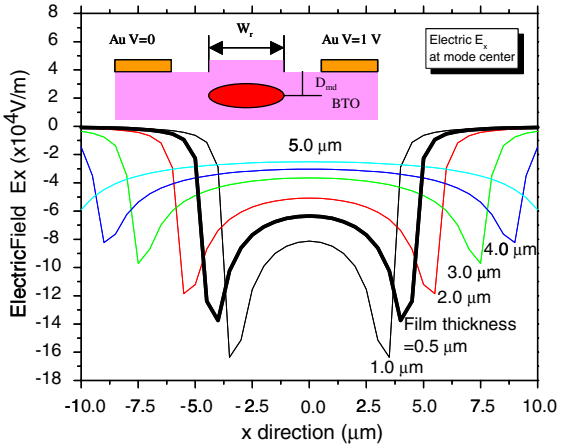

Fig. 4. The electric field E_x along the x-axis for the six different values of the film thickness (0.5–5.0 μm) with optimal waveguide designs when a voltage of 1.0 V is applied. The gap G between electrodes is set as $2W_{D5\%}$.

2.3. Electric field strength and overlap integral factor

To achieve electro-optic modulation, an electric field is first produced by the applied voltage V to the $BaTiO_3$ thin-film waveguide shown in Fig. 4. The electric field induces a change in the refractive index of the optical mode in the waveguide, resulting in an optical phase shift. The MZI geometry then transfers the phase shift to intensity change. The intensity modulation is dependent on the EO coefficient r_{eff} (here it is r_{51}) as well as the strength of the electric field. We calculate the horizontal component of the electric field distribution (x-direction of the system) for the six film thickness values with the optimal waveguide designs by taking the gap $G = 2W_{D5\%}$ and obtain the results of the electric field strength E_x at the mode center located at $z = -D_{md}$ as shown in Fig. 4. The electric field strength gradually decreases with increasing thickness of $BaTiO_3$ film because the optical mode center gradually moves down with increasing $BaTiO_3$ film thickness. We obtained the overlap integral factors Γ for the six film thickness values with optimal waveguide designs, which are shown in Table 2. We see that the electric field

Table 2
Electric field value at the mode center and electrical/optical overlap integral factor value at the optimal points for the six values of $BaTiO_3$ film thickness: 0.5–5.0 μm

Items	0.5 (μm)	1.0 (μm)	2.0 (μm)	3.0 (μm)	4.0 (μm)	5.0 (μm)
E_x ($\times 10^4$ V/m)	−6.3490	−8.1330	−5.0830	−3.6555	−3.0296	−2.5097
E/O overlap	0.5664	0.5720	0.5635	0.5595	0.5560	0.5539

strength increases substantially in a thinner film. The larger the optical effective refractive index (or propagating refractive index), potentially the closer the matching of the optical effective refractive index with the RF microwave effective refractive index, a requirement for achieving velocity matching between the optical and microwave fields. The increase in the microwave effective refractive index (hereafter referred to as RF effective refractive index) with the thickness of the $BaTiO_3$ films increases is faster than that of the optical effective refractive index, and in some cases might lower the amount of velocity matching instead, resulting in a net advantage for thinner films.

2.4. Calculations for $V_\pi^2 L$

From Eq. (2), we see that a large EO coefficient r_{51} will strongly reduce $V_\pi^2 L$, as will a large overlap integral factor Γ and a small electrode gap G. The $V_\pi^2 L$ can also be reduced in other ways, such as by varying the ratio of the ridge height to the film thickness [2–4]. The effective EO coefficient r_{eff} is dependent on the EO properties of materials and the crystalline direction. An ideal $BaTiO_3$ film can have an EO coefficient of $r_{51} = 730$ pm/V [6]. EO coefficients in early experimental films were estimated to be around 35 pm/V [7,8], and they have been improved recently [14]. Our simulations of $V_\pi^2 L$ for the EO modulator regime are performed with the experimental film and the ideal film, respectively, and the results are shown in Table 3(a) and (b), respectively. These simulations are done for the six different thickness values of $BaTiO_3$ films with the optimal waveguide designs given in Table 1 with $G = 2W_{D5\%}$. Note that as expected, the $V_\pi^2 L$ value increases with the thickness of the $BaTiO_3$ films. For the purposes of this comparative study, we assume that the experimental film has the same dielectric constants as the ideal film, with $\varepsilon_x = 2200$ and $\varepsilon_z = 56$.

3. Study for matching condition and frequency response

3.1. Principle

The 3 dB frequency response of an EO intensity modulator is given by [3]:

$$m(f) = \left[\frac{1 - 2e^{-\alpha L}\cos 2u + e^{-2\alpha L}}{(\alpha L)^2 + (2u)^2}\right]^{1/2}, \tag{4a}$$

$$u = \pi f L(N_{\text{rf}} - N_{\text{op}})/c, \tag{4b}$$

where α is the microwave RF propagation loss coefficient, c is the velocity of light in vacuum, L is the interaction length (i.e., the electrode length), and N_{op} and N_{rf} are the effective indices of the optical wave and microwave, respectively. The absolute value of $|N_{\text{rf}} - N_{\text{op}}|$ indicates the amount of velocity matching between the microwave and optical wave. If this velocity matching condition is completely satisfied, i.e., $|N_{\text{rf}} - N_{\text{op}}| = 0$, in the case where RF propagation loss $\alpha = 0$, the 3 dB frequency response will become infinitely large in Eq. (4). In fact, it is difficult to have complete velocity matching because $BaTiO_3$ has relatively large microwave dielectric constants. Even if the velocity matching condition is completely satisfied, other factors such as the microwave propagation

Table 3
$V_\pi^2 L$ values of the (a) ideal and (b) experimental film case for the six values of $BaTiO_3$ film thickness: 0.5–5.0 μm and $G = 2W_{D5\%}$ with the optimal waveguide designs, and the corresponding values of L for $V_\pi = 5V$

Items	0.5 (μm)	1.0 (μm)	2.0 (μm)	3.0 (μm)	4.0 (μm)	5.0 (μm)
(a) Ideal film						
$V_\pi^2 L$ (V^2 cm): $r_{51} = 730$ pm/V	1.75	2.05	2.71	5.22	7.62	11.05
L (cm): $V_\pi = 5$ V	0.07	0.04	0.11	0.21	0.30	0.44
(b) Experimental film						
$V_\pi^2 L$(V^2 cm): $r_{\text{exp}} = 35$ pm/V	110.0	126.3	170.6	328.7	479.7	696.0
L (cm): $V_\pi = 5$ V	4.4	2.64	6.82	13.15	19.19	27.84

attenuation can strongly affect the 3 dB frequency response of the modulator system when the device length is long [1–3,15].

The characteristic impedance Z_m needs match the external microwave generator impedance (typically 50 Ω) to minimize reflected power. The characteristic impedance Z_m can be calculated via [3]

$$Z_m = \frac{1}{c\sqrt{CC_0}}, \quad (5)$$

where C is the capacitance of the EO modulator system and C_0 is the capacitance value when all the dielectric materials in this system are replaced by air. Characteristic impedance Z_m is generally determined by both the microwave electrodes and the waveguide geometry, and can be altered by changing the geometrical structure of the EO modulators.

3.2. Simulation for Z_m

Using Eqs. (3) and (5), we obtain the simulation results of Z_m for all six thickness values of the $BaTiO_3$ films from 0.5 to 5.0 μm assuming the optimal waveguide designs shown in Table 1. The results are shown in Table 4(a). For the simulation, we selected the electrode thickness T_m to be 0.5 μm and the middle electrode width W_m to be 8.0 μm. The gap G between two electrodes is set as $G = 2W_{D5\%}$. We find that the characteristic impedance of the $BaTiO_3$/MgO based EO modulators is generally small (20–25 Ω), in comparison to the typical 50 Ω required. In order to increase the characteristic impedance, we changed the gap G to $G = 2W_{D5\%} + 24.0$ μm, and obtained the higher characteristic impedance values shown in Table 4(b). Note that the characteristic impedance of the system has been increased from about 20–25 Ω to about 40–50 Ω. In particular, the value of Z_m is increased from 25 to 52 Ω at the film thickness of 0.5 μm, which is close to the typical matching condition of system characteristic impedance. However, the corresponding $V_\pi^2 L$ values also increase as shown in Table 5(a), and the comparative values of $V_\pi^2 L$ for the experimental film are shown in Table 5(b). On the average, the $V_\pi^2 L$ values are increased by 40 times for the experimental film with $r_{exp} = 35$ pm/V and the ideal film with $r_{51} = 730$ pm/V, respectively, after the gap between electrodes is changed from $G = 2W_{D5\%}$ to $G = 2W_{D5\%} + 24.0$ μm. As we know, the increase in $V_\pi^2 L$ values will require an increase in the interaction length for the same drive voltage. According to Eq. (4), this will further decrease the 3 dB frequency response. The results also show that Z_m can become smaller with the increase in the $BaTiO_3$ film thickness.

4. Frequency response

4.1. Microwave conductor propagation loss

In high-speed EO intensity modulators, the modulating electric fields are microwave signals which experience attenuation induced by both the resistance of the metallic conductor due to reduced skin penetration depth at high frequency and the dielectric propagation losses [1]. In particular, the conductor propagation loss plays a dominant role in the 3 dB frequency response. Generally, the conductor propagation loss cannot be ignored when the frequency response is higher than 10 GHz in conventional $LiNbO_3$ modulators. The conductor propagation loss coefficient α_c is expressed as [3]

Table 4
Z_m for the six values of $BaTiO_3$ film thickness (0.5–5.0 μm) when G is set at (a) $2W_{D5\%}$ and (b) $2W_{D5\%} + 24.0$ μm with the optimal waveguide designs

Items	0.5 (μm)	1.0 (μm)	2.0 (μm)	3.0 (μm)	4.0 (μm)	5.0 (μm)
(a) $2W_{D5\%}$						
Z_m	25	19	20	21	21	21
(b) $2W_{D5\%} + 24.0$ μm						
Z_m	52	45	38	36	35	35

Table 5
$V_\pi^2 L$ values of the (a) ideal and (b) experimental film case for the six values of $BaTiO_3$ film thickness: 0.5–5.0 μm and $G = 2W_{D5\%} + 24.0$ μm with the optimal waveguide designs, and the corresponding values of L for $V_\pi = 5$ and 10 V

Items	0.5 (μm)	1.0 (μm)	2.0 (μm)	3.0 (μm)	4.0 (μm)	5.0 (μm)
(a) Ideal film						
$V_\pi^2 L$ (V^2 cm) : $r_{51} = 730$ pm/V	71.7	65.6	78.0	90.6	100.8	113.0
L (cm): $V_\pi = 5$ V	2.88	2.63	3.12	3.62	4.03	4.52
L (cm): $V_\pi = 10$ V	0.72	0.66	0.78	0.91	1.01	1.13
(b) Experimental film						
$V_\pi^2 L$ (V^2 cm) : $r_{exp} = 35$ pm/V	4515	4133	4908	5705	6346	7117
L (cm): $V_\pi = 5$ V	180.6	165.3	196.3	228.2	253.8	284.7
L (cm): $V_\pi = 10$ V	45.2	41.3	49.1	57.1	61.0	71.2

Table 6
Performance of typical regimes of EO intensity modulator with the ideal films of $BaTiO_3$: 0.5–5.0 μm when $G = 2W_{D5\%} + 24.0$ μm

Items	0.5 (μm)	1.0 (μm)	2.0 (μm)	3.0 (μm)	4.0 (μm)	5.0 (μm)
N_{op}	2.0466	2.1714	2.2503	2.2711	2.2782	2.2821
N_{rf}	4.4725	5.4422	6.9841	8.1542	9.1829	9.9104
$\alpha_{0(dB/GHz^{0.5}cm)}$	1.96	2.25	2.69	2.86	2.98	2.98

$$\alpha_c = \frac{R_s}{2Z_0 Z_m} \frac{\partial Z_{m0}}{\partial \vec{n}}, \tag{6}$$

where R_s is the surface resistance of the electrode, Z_0 the impedance of free space, Z_{m0} the free-space characteristic impedance of electrode and $\partial Z_{m0}/\partial \vec{n}$ indicates the derivative of Z_{m0} with respect to the incremental recession of the electrode surfaces.

4.2. Calculation for the frequency response

In this section, we will consider designs for both the cases where $Z_m = 50\ \Omega$ and $Z_m = 25\ \Omega$, respectively, for the calculation of device performance. The main parameters of interest are the 3 dB frequency response, the conductor propagation loss, and the RF effective refractive index. For the experimental $BaTiO_3$ films, only the velocity matching limitation is considered in the calculation for the 3 dB frequency response and the velocity limited frequency response is expressed by Δf_vel. But, for the ideal $BaTiO_3$ films, both the velocity matching factor and microwave attenuation induced by the conductor propagation loss are considered and the velocity/loss limited frequency response is expressed by Δf_vel/loss.

Using Eqs. (3), (5), and (6), we first simulate some important parameters of the waveguide EO intensity modulators for the six thickness values of $BaTiO_3$ thin-films shown in Table 1. Table 6 summarizes the simulation results when the gap G between the two electrodes is set at $2W_{D5\%} + 24.0$ μm ($Z_m \approx 50\ \Omega$ case). Note from Table 6 that the RF effective refractive index reduces rapidly from 9.91 to 4.47 when the thickness of the $BaTiO_3$ film decreases from 5.0 to 0.5 μm, while the optical effective refractive index remains around 2.0–2.3. In order to study the effects of the velocity matching condition and conductor propagation loss on the frequency response of EO modulators, we chose two typical driving voltage of $V_\pi = 5.0$ V and $V_\pi = 10.0$ V to simulate the most important performance of EO modulators, the frequency response for the ideal film having $r_{51} = 730$ pm/V, and obtain the results as shown in Fig. 5(a). The comparative results for film having $r_{eff} = 35$ pm/V are obtained as shown in Fig. 5(b). The frequency responses in Fig. 5 were obtained by fitting the respective values of interaction length L by using the $V_\pi^2 L$ shown in

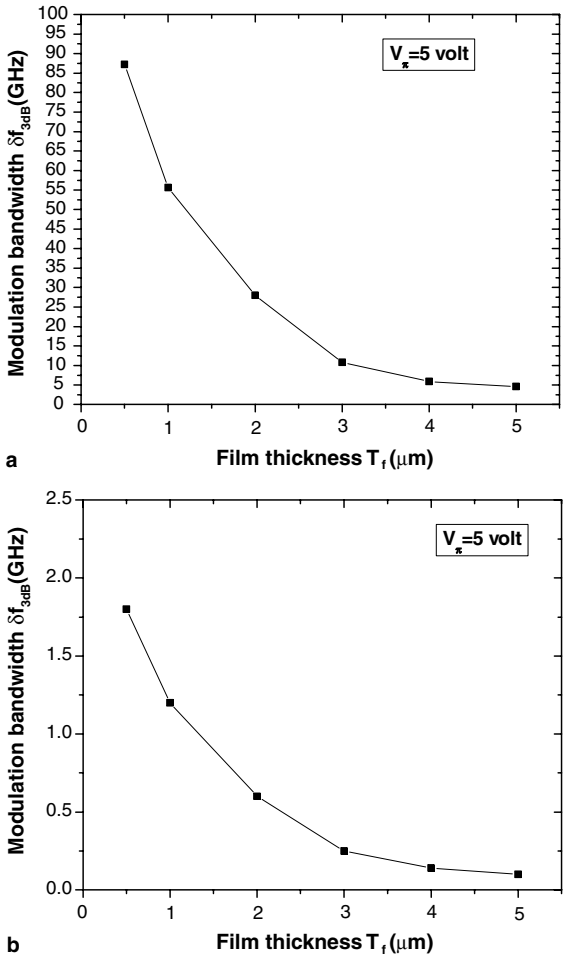

Fig. 5. 3 dB frequency response vs. film thickness with the ideal film and the experimental film: (a) the ideal film and (b) the experimental film, where $T_m = 0.5$ μm, $W_m = 8.0$ μm, $W_s = 15.0$ μm, $G = 2W_{D5\%}$ μm at $V_\pi = 5$ V.

Tables 5(a) and (b), respectively. Note that increasing the electrode gap for better matching the characteristic impedance with that of outside RF generator system further limits the frequency–voltage-length performance of the EO modulator. Both Table 6 and Fig. 5 show an optimal thickness of 0.5 μm of films. For instance, when the film thickness reduces from 5 to 0.5 μm, with a drive voltage of 5 V, the frequency response of the experimental film case increases from 0.1 to 1.8 GHz and that of the ideal film case increases from 4.6 to 87 GHz due to the gradually improved velocity matching condition between the light wave and microwave. We see from the above results that the effective RF refractive index of thin $BaTiO_3$ films can be relatively lower compared to the bulk case, which helps to reduce the velocity mismatch and increase the frequency response substantially [7]. Next we select the case $G = 2W_{D5\%}$ ($Z_m = 25\ \Omega$) to investigate the EO modulator frequency performance as a function of such electrode geometries as the thickness of each electrode, and the electrode gap G. It turns out that besides the characteristic impedance Z_m of the electrodes and the RF propagation loss α, the RF effective refractive index N_{rf} is also dependent on the geometrical structure of the electrodes and they further impact the frequency response of the EO modulator [4].

The $Z_m \approx 25\ \Omega$ case may not be typical, but it can be used if the voltage source is designed to match 25 Ω. In Fig. 6, we consider the case of $Z_m \approx 25\ \Omega$ with $G = 2W_{D5\%}$ for the 0.5 μm thick $BaTiO_3$ thin-film under the half-wave drive voltage of 5.0 V and, respectively, show the RF effective refractive index N_{rf} (Fig. 6(a)), the microwave propagation attenuation coefficient α_c (Fig. 6(b)) due to conductor absorption and the frequency response $\delta f_{3\,dB}$ (Fig. 6(c)) as functions of the electrode thickness. We find that the modulation frequency becomes substantially higher. Note that both the RF effective refractive index and the microwave propagation attenuation coefficient are gradually improved with the increase of electrode thickness. As a result, the frequency responses approach more desirable values with the increase of electrode thickness. For the case that both the phase velocity match and the microwave propagation attenuation are considered under a drive voltage of 5 V, $\delta f_{3\,dB}$ is 87 GHz for 0.5 μm thick electrodes, and it increases to 112 GHz for 6.0 μm thick electrodes. We simulate the relations between the modulation bandwidth and the half-wave drive voltage as shown in Fig. 7. In this simulation, two cases are considered. In one case, both the phase velocity match and the RF wave propagation attenuation are considered in simulation, while for the other case only the phase velocity match is considered in simulation.

In Table 7, we summarize the voltage and frequency performance for the $Z_m \approx 25\ \Omega$ case with 6.0 μm thick electrodes. We see that at 4.8 V drive

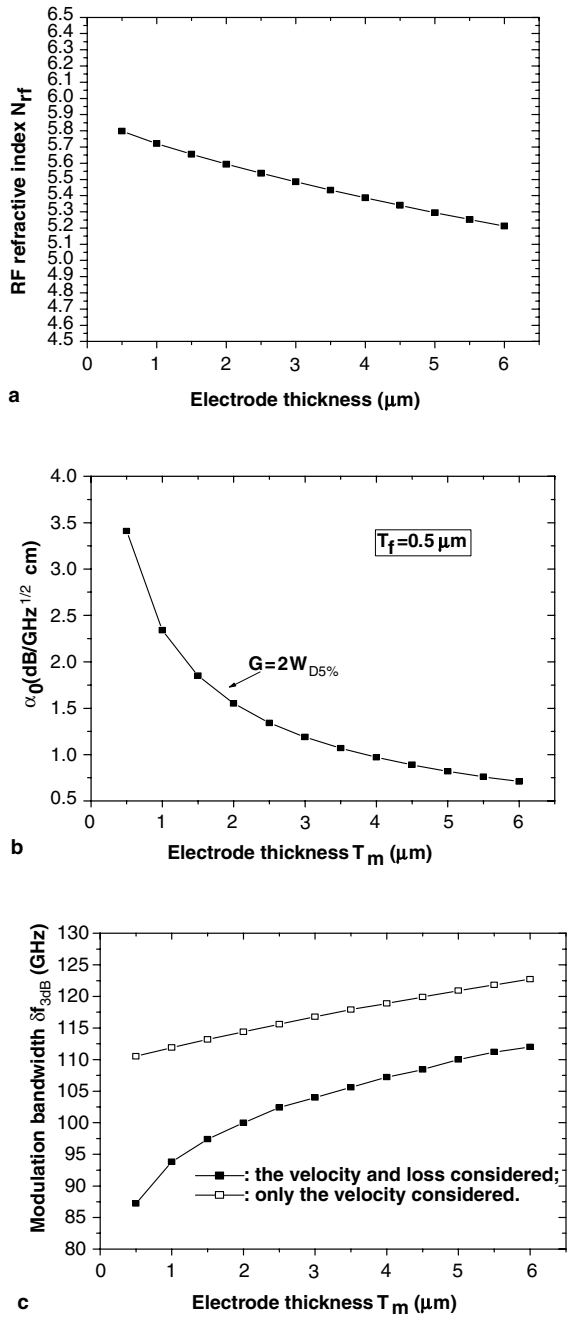

Fig. 6. RF refractive index, microwave propagation attenuation coefficient and 3 dB frequency response vs. electrode thickness: (a) RF refractive index, (b) microwave propagation attenuation coefficient and (c) 3 dB frequency response with the ideal film and the shorter $L = 1.45$ mm at 5.0 V V_π, where $T_f = 0.5$ μm, $W_m = 8.0$ μm, $W_s = 15.0$ μm, $G = 2W_{D5\%}$ μm.

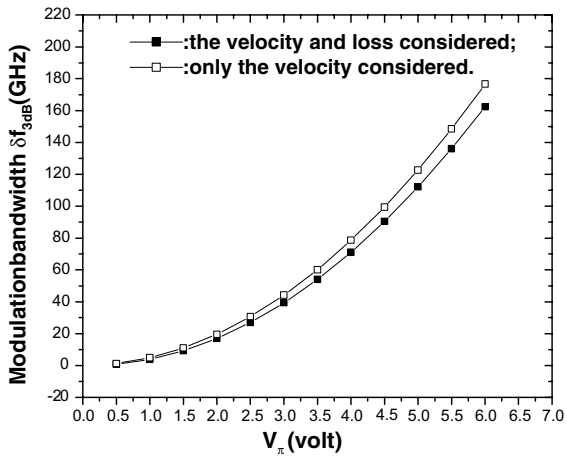

Fig. 7. 3 dB frequency response vs. half-wave drive voltage with the ideal film where $T_f = 0.5$ μm, $T_m = 6.0$ μm, $W_m = 8.0$ μm, $W_s = 15.0$ μm, $G = 2W_{D5\%}$ μm.

voltage, the modulator bandwidth is 100 GHz; at 3.0 V drive voltage the modulator bandwidth can be 40 GHz; the modulator bandwidth of 10 GHz can be obtained with a low drive voltage of 1.5 V, and a modulator bandwidth of 2.5 GHz can still be obtained with a low drive voltage of 0.75 V. The device lengths for these four cases are 0.5, 1.9, 7.8, and 31.1 mm, respectively. This is favorable compared with a typical commercial $LiNbO_3$ based EO modulator having 10 GHz modulation bandwidth with 3.5 V V_π, 40 GHz modulation bandwidth with 5.0 V V_π. Table 7 also shows the RF wavelength at the modulation bandwidth. We also find that although the modulator is only a millimeter long, its size is still large compared with its RF wavelength. This is because of the large ε value of $BaTiO_3$ giving much shorter RF wavelength. Our study here shows that although the $G = 2W_{D5\%}$ (25 Ω) case has a higher N_{rf} than the $G = 2W_{D5\%} + 24.0$ (50 Ω) case at the same value of electrode thickness, the modulation bandwidth is higher for $Z_m \approx 25$ Ω at the same drive voltage. This is because of the shorter modulator length required for the $Z_m \approx 25$ Ω case. In order to see whether the velocity matching factor or the RF propagation loss factor is the main contributing factor to the change in the modulation bandwidth, we study the case where the RF propagation loss is set to be zero. We obtained the re-

Table 7
Frequency response for EO modulator based on ideal film at four V_π values (the electrode thickness = 6.0 μm, the film thickness = 0.5 μm, and $G = 2W_{D5\%}$)

Half-wave voltage V_π (V)	0.75	1.5	3.0	4.8
Frequency response δf (GHz) (λ_{RF} in mm)	2.5 (19.2)	10 (4.5)	40 (1.2)	100 (0.5)
Electrode L (mm)	31.1	7.8	1.9	0.8

Table 8
Four typical values of modulation bandwidth of the EO modulator for analyzing the influences of the RF refractive index and the RF propagation loss ($V_\pi = 5.0$ V and $G = 2W_{D5\%}$)

Electrodes thickness (μm)	Δf_vel at $\alpha = 0$ (GHz)	Δf_vel/loss (GHz)
0.5	110.5	87.2
6.0	122.7	112.0

sults for the frequency response at two values, 0.5 and 6.0 μm, of electrode thickness under a drive voltage of 5 V as summarized in Table 8. Note from Table 8 that the change in modulation bandwidth due to N_{rf} (from 110 GHz to 123 GHz) is close to that due to the microwave propagation loss (from 123 to 112 GHz). Therefore the improvement in the modulation bandwidth with thicker electrodes is about half due to the reduced RF loss and half due to improved velocity matching as the thicker electrodes lead to lower RF effective refractive index.

5. Conclusion

We investigated the performance of EO modulators based on thin-film $BaTiO_3$ grown on an MgO substrate. We demonstrated the feasibility of the fabrication of EO modulators with such performance parameters as low drive voltage, short device interaction length, and high-frequency response. We used numerical examples based on an experimental thin-film and an ideal thin-film of $BaTiO_3$ for a wide range of film thickness values (0.5–5.0 μm). First, the influence of the film thickness on the special relation of the half-wave drive voltage and the interaction length $V_\pi^2 L$ is studied. We found that the $V_\pi^2 L$ value increases with the thickness of the film. In the second stage of this work, two matching conditions for high-speed EO modulation, velocity matching and the characteristic impedance matching, were studied. The performance of an EO intensity modulator with a $BaTiO_3$ thin-film strongly depends on the film thickness. We showed that the RF effective refractive index of the EO modulator system decreases with decreasing thickness of the $BaTiO_3$ films. For 0.5 μm thick ideal thin-film with $r_{51} = 730$ pm/V, a modulation bandwidth of >100 GHz with a drive voltage of 4.8 V and device length of 0.8 mm, >40 GHz with a low drive voltage of 3.0 V and device length of 1.9 mm, >10 GHz with a low drive voltage of 1.5 V and device length of 7.8 mm, and >2.5 GHz with a low drive voltage of 0.75 V and device length of 31.1 mm can be achieved. In these analyses, no buffer layer is used for reducing the microwave RF effective refractive index, which could be used to further fine-tune the trade-off between the modulator frequency response and switching voltage.

Acknowledgments

The authors gratefully acknowledge the funding of the research by the MRSEC program of the National Science Foundation (DMR-0076097) at Northwestern University and the 100-Person-Plan Program of the Chinese Academy of Sciences.

References

[1] N. Dagli, IEEE Trans. Microwave Theory Tech. MTT-47 (7) (1999) 1151.
[2] N. Anwar, C. Themistos, B.M. Azizur, K.T.V. Grattan, J. Lightwave Technol. 17 (4) (1999) 598.
[3] S. Haxha, B.M.A. Rahman, K.T.V. Grattan, Appl. Opt. 42 (15) (2003) 2674.
[4] R.C. Alferness, IEEE Trans. Microwave Theory Tech. MTT-30 (8) (1982) 1121.

[5] R.L. Holman, L.A. Johnson, D.P. Skinner, Opt. Eng. 26 (1) (1987) 134.
[6] M. Zgonik, P. Bernasconi, M. Duelli, R. Schlesser, P. Gunter, M.H. Garret, D. Rytz, Y. Zhu, X. Wu, Phys. Rev. B 50 (9) (1994) 5941.
[7] D.M. Gill, C.W. Conrad, G. Ford, B.W. Wessels, S.T. Ho, Appl. Phys. Lett. 71 (13) (1997) 1783.
[8] S.S. Kim, D. Towner, A. Teren, B.W. Wessels, S.-S. Chang, S.-T. Ho, OSA Integrated Photonics Research Topical Meeting, IWB1, 2001.
[9] A. Petraru, J. Schubert, M. Schmid, Ch. Buchal, Appl. Phys. Lett. 81 (8) (2002) 1375.
[10] A. Petraru, J. Schubert, M. Schmid, O. Trithaveesak, Ch. Buchal, Opt. Lett. 28 (24) (2003) 2527.
[11] F. Abdi, M.D. Fontana, M. Aillerie, G. Godefroy, Ferroelectrics 133 (1992) 175.
[12] M. Minakata, SPIE Proc. (Invited Paper) 4532 (2001) 16.
[13] H. Jin, M. Belanger, Z. Jakubczyk, IEEE Quantum. Electron. QE-27 (2) (1991) 243.
[14] Pingsheng Tang, D.J. Towner, A.L. Meier, B.W. Wessels, Appl. Phys. Lett. 85 (20) (2004) 4615.
[15] O. Mitomi, K. Noguchi, H. Miyazawa, IEEE Trans. Microwave Theory Tech. MTT-43 (9) (1995) 2203.